

## Continuous-wave light modulation at molecular frequencies

J. T. Green, J. J. Weber, and D. D. Yavuz

*Department of Physics, 1150 University Avenue, University of Wisconsin at Madison, Madison, Wisconsin 53706, USA*

(Received 18 March 2010; published 26 July 2010)

By using continuous-wave (CW)–stimulated Raman scattering inside a high-finesse cavity, we generate three CW spectral components covering about one octave of optical bandwidth. We investigate the mutual coherence of these three beams by studying phase-dependent second harmonic generation. From the high contrast of the observed interference fringes, we infer very good phase coherence across the spectrum and thereby infer the synthesis of a near single-cycle optical wave form.

DOI: [10.1103/PhysRevA.82.011805](https://doi.org/10.1103/PhysRevA.82.011805)

PACS number(s): 42.65.Dr, 42.50.Gy, 42.65.Re

It is well known that when light is modulated, it typically produces three equally spaced frequencies: one carrier and two sidebands. These frequencies can be used, for example, to synthesize frequency-modulated (FM) or amplitude-modulated (AM) temporal wave forms, depending on their relative phase. Light can be modulated at rates exceeding 10 GHz using nonlinear optical effects such as electro-optic light modulation. Modulating light at much higher rates has proved to be difficult. It was only in 2001, more than four decades after the invention of the laser, that light modulation at molecular frequencies was demonstrated using Q-switched (nanosecond-pulsed) spectral components [1]. In this article, we extend this idea to the continuous-wave (CW) domain and demonstrate CW light modulation at a frequency of 90 THz. The modulation frequency in our experiment is about one third of the optical carrier frequency.

Our experiment builds on the pioneering work of Carlsten and colleagues, who were the first to demonstrate stimulated Raman scattering in gases with CW laser beams [2–4]. In stimulated Raman scattering, molecules pumped with sufficiently intense light at frequency  $\omega_p$  produce Stokes light at  $\omega_s = \omega_p - \omega_v$ , where  $\omega_v$  is the selected vibrational or rotational frequency of the molecule. If the molecules are placed inside a cavity with a high finesse at the pump and at the Stokes wavelengths, efficient Stokes generation in molecular gases can be achieved with CW laser beams. Advances in high-reflectivity, ultralow-loss dielectric coatings have allowed efficient Stokes generation with pump laser powers as low as 1 mW. Both rotational and vibrational CW Stokes sideband generation has been reported. The key difference of our work when compared with earlier experiments is that we drive a sufficiently large molecular coherence such that we not only generate the Stokes beam but also produce substantial anti-Stokes light at a frequency of  $\omega_a = \omega_p + \omega_v$ . The anti-Stokes beam is produced by a single pass through the system: that is, the cavity does not have a high finesse at the anti-Stokes wavelength. Specifically, by using the fundamental vibrational transition in molecular deuterium ( $D_2$ ), we produce a CW spectrum with three discrete components at wavelengths 1.56  $\mu\text{m}$ , 1.06  $\mu\text{m}$ , and 807 nm. These wavelengths span 0.95 octaves of optical bandwidth. We then show that these beams have almost perfect mutual-phase coherence and thereby infer the synthesis of a near single-cycle optical wave form.

Our work has largely been motivated by the technique of adiabatic Raman generation at maximum coherence, which has been pioneered by Harris and Sokolov [5,6]. As mentioned

previously, about nine years ago, this technique allowed the first light modulation at molecular frequencies. Building on this work, Shverdin *et al.* and Kung and colleagues have synthesized the first single-cycle optical pulses [7,8]. Recently, the synthesis of arbitrary optical wave forms using a broad Raman spectrum has also been demonstrated [9]. We view our experiment as the first step toward extending these pioneering efforts to the CW domain. In the future, by generating more than three spectral components, our technique may allow arbitrary wave-form synthesis with CW laser beams. In other related prior work, the use of stimulated Raman scattering for ultrashort-pulse synthesis was originally suggested by Imasaka and colleagues [10] and by Kaplan [11]. Hakuta and colleagues have produced a broad Raman spectrum by using solid molecular hydrogen [12]. Katsuragawa and coworkers have demonstrated an octave-spanning Raman comb with carrier-envelope phase control [13]. Utilizing an impulsive Raman excitation technique, Korn and colleagues have produced optical pulses as short as 3.8 fs [14]. Over the past decade, there has also been significant progress on CW-stimulated Raman scattering. Zaitsev *et al.* have demonstrated efficient CW rotational Raman generation at the anti-Stokes wavelength by tuning the cavity resonances with the help of a dispersive gas [15]. The same group has also demonstrated the generation of a second rotational Stokes beam through cascade-stimulated Raman scattering [16]. Couny and coworkers have demonstrated CW rotational Stokes output power of more than 2 W inside a hollow photonic crystal fiber [17]. We have recently demonstrated high-power CW rotational Raman generation at low gas pressures in molecular  $D_2$  [18].

We proceed with a detailed description of our experiment. As shown in Fig. 1, the experiment is performed at room temperature inside a cavity with a high finesse at the pump (1.064- $\mu\text{m}$ ) and the Stokes (1.56- $\mu\text{m}$ ) wavelengths. The high-finesse cavity (HFC) is placed inside a vacuum chamber that we fill with  $D_2$ . The mirrors of the cavity have ultralow-loss, high-reflectivity dielectric coatings with a CW optical damage threshold exceeding 20 MW/cm<sup>2</sup>. The total scattering, absorption, and transmission losses of the mirrors at the two wavelengths are at the level of 100 parts per million (ppm). The mirrors have a radius of curvature of 50 cm, and the length of the cavity is 27 cm. The free spectral range of the cavity is 555 MHz. The calculated finesse of the cavity at the two wavelengths is about 22,000 resulting in a full width at half maximum (FWHM) cavity resonance linewidth of 25 kHz. One of the mirrors is mounted on a piezo-electric

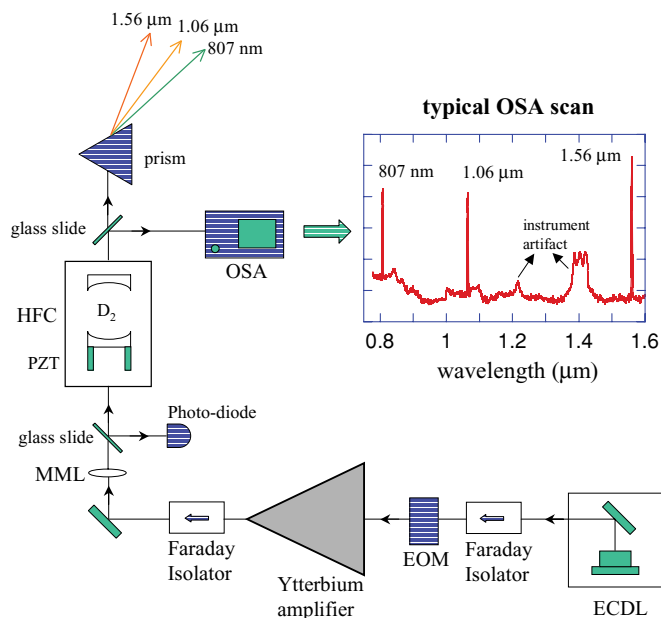


FIG. 1. (Color online) The setup of our experiment. The experiment starts with an external cavity diode laser at a wavelength of  $1.064 \mu\text{m}$ . The laser beam is amplified to a high-CW power level with a ytterbium fiber amplifier. When we lock the high-power pump beam to the cavity, we observe the generation of Stokes and anti-Stokes sidebands at wavelengths of  $1.56 \mu\text{m}$  and  $807 \text{ nm}$  respectively. The plot shows a typical spectrum that we observe on an optical spectrum analyzer (the vertical scale is logarithmic). The marked structures in the plot are due to an instrument artifact. ECDL, external cavity diode laser; EOM, electro-optic modulator; MML, mode-matching lens; HFC, high-finesse cavity; PZT, piezo-electric transducer; and OSA, optical spectrum analyzer.

transducer (PZT) to allow for slight adjustments of the cavity length.

To produce the desired high-power pump laser beam, we start with an external cavity diode laser (ECDL) at a wavelength of  $1.064 \mu\text{m}$ . The ECDL is custom built with an optical power of  $20 \text{ mW}$  and a free running linewidth of about  $0.5 \text{ MHz}$ . After a Faraday isolator, the beam goes through an electro-optic modulator (EOM). The EOM puts  $50\text{-MHz}$  phase modulation on the input beam, which is used to lock the laser to the HFC. We then amplify the beam to a CW power of  $20 \text{ W}$  with a ytterbium fiber amplifier. The  $20\text{-W}$  output beam is linearly polarized and coupled to the  $\text{TEM}_{00}$  mode of the HFC using a mode-matching lens (MML). We use the Pound-Drever-Hall technique to lock the pump laser to the cavity [19]. We detect the reflected beam from the input cavity mirror with a photodiode and generate two separate feedback signals. The first (fast) feedback modifies the ECDL current, while the second (slow) feedback makes adjustments to the cavity PZT.

When we lock the pump laser to the cavity, we observe CW Raman lasing of the Stokes beam. The Raman lasing occurs on the  $|\nu = 0, J = 0\rangle \rightarrow |\nu = 1, J = 0\rangle$  fundamental vibrational transition of  $\text{D}_2$  at a transition frequency of  $2994 \text{ cm}^{-1}$  ( $89.8 \text{ THz}$ ). The pump beam at a wavelength of  $1.064 \mu\text{m}$  produces the Stokes beam at a wavelength of  $1.56 \mu\text{m}$ . The intense pump and Stokes beams inside the cavity drive the

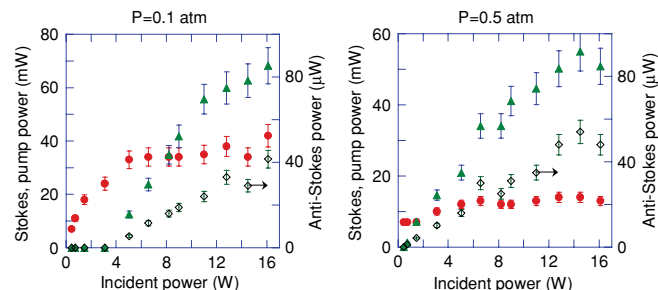


FIG. 2. (Color online) The optical power in the Stokes (triangles), pump (circles), and anti-Stokes (diamonds) beams at two different  $\text{D}_2$  pressures:  $P = 0.1 \text{ atm}$  and  $P = 0.5 \text{ atm}$ . Although we observe a significantly reduced Raman generation threshold at  $P = 0.5 \text{ atm}$ , the maximum generated powers in the Stokes and anti-Stokes beams are comparable for the two pressures.

molecular coherence and generate the anti-Stokes beam at a wavelength of  $807 \text{ nm}$  through four-wave mixing. The cavity mirrors do not have a high reflectivity at  $807 \text{ nm}$ , and the anti-Stokes light is generated through a single pass. After the cavity, we separate out the three beams with the use of an SF11 equilateral prism and perform our measurements.

Figure 2 shows the measured power after the prism in each of the three beams as the incident pump power is varied for two different gas pressures:  $P = 0.1 \text{ atm}$  and  $P = 0.5 \text{ atm}$ . These pressures are more than an order of magnitude lower than typical pressure values used in CW-stimulated Raman scattering [2–4]. For  $P = 0.1 \text{ atm}$ , we observe a lasing threshold of  $3 \text{ W}$ , and for the highest incident power we generate  $68 \text{ mW}$  of Stokes,  $42 \text{ mW}$  of pump, and  $41 \mu\text{W}$  of anti-Stokes light. For  $P = 0.5 \text{ atm}$ , the lasing threshold drops to  $0.6 \text{ W}$ , and we generate maximum powers of  $55 \text{ mW}$ ,  $14 \text{ mW}$ , and  $54 \mu\text{W}$  in the three beams respectively.

To check the mutual coherence of these three beams, we study nonlinear generation with a  $\chi^{(2)}$  process in an ultrathin ( $10 \mu\text{m}$ )  $\beta$ -barium-borate (BBO) crystal [20]. Figure 3 shows the experimental schematic. After we separate out the beams, we reflect and recombine them with three independent mirrors. The three beams are then focused to the BBO crystal with an achromatic-doublet lens. An ultrathin crystal is needed to avoid any phase slips between the three beams due to dispersion while propagating through the crystal. The alignment of the three beams at the focus is achieved by optimizing transmission through a small pinhole. Through the second-order  $\chi^{(2)}$  nonlinearity of the crystal, we generate green light at a wavelength of  $532 \text{ nm}$ . As shown in the inset of Fig. 3, there are two different quantum mechanical processes that can generate  $532\text{-nm}$  light: two photons from the pump beam (second harmonic generation) or one photon each from the Stokes and anti-Stokes beams (sum-frequency generation). Depending on the relative phase difference between the three Raman beams, these two paths may interfere constructively or destructively. Since the absolute frequencies of the beams are not multiples of their frequency difference, there is only one well-defined relative phase [1]. We adjust this phase by inserting a  $1\text{-mm}$ -thick BK7 glass slide in the beam path of the  $1.56\text{-}\mu\text{m}$  Stokes beam. Rotating the slide changes the optical beam path and thereby modifies the phase.

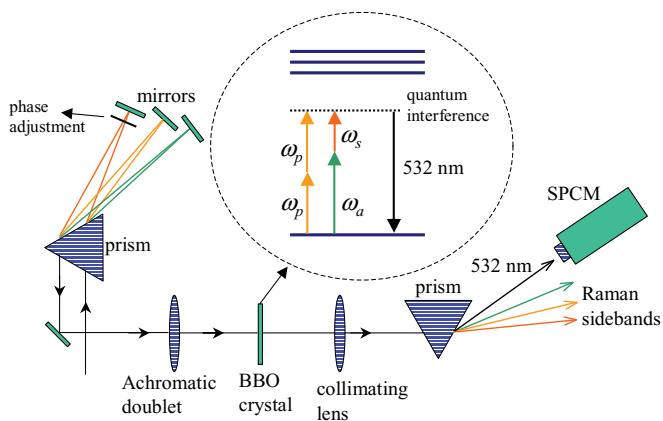


FIG. 3. (Color online) Phase-dependent second harmonic generation using the Raman spectrum. Through the second-order nonlinearity of the BBO crystal, we generate green light at a wavelength of 532 nm. We spatially separate the 532-nm light and detect it using a single-photon counting module (SPCM). As shown in the inset, there are two paths that can generate 532-nm light in the BBO crystal: pump + pump (second harmonic generation) and Stokes + anti-Stokes (sum-frequency generation). Depending on the relative phase between the three incident beams, these paths can interfere constructively or destructively.

After the BBO crystal, we spatially separate out the 532-nm beam with a prism and detect it using a single-photon counting module (SPCM). We block stray light with the use of a narrowband interference filter that is placed in front of the SPCM. Figure 4 shows the number of photons per second detected at the SPCM as a function of the introduced phase change. We calculate the phase change from the exact parameters of the slide (the refractive index and the rotation angle). In this experiment, to make the interfering paths more comparable in amplitude, we attenuate the pump beam by 60% with a neutral density filter. The measured power values before the BBO crystal in each beam are 39.4 mW (Stokes), 5.61 mW (pump), and 38  $\mu$ W (anti-Stokes). The measured beam sizes (Gaussian waist) for the three beams at the focus are

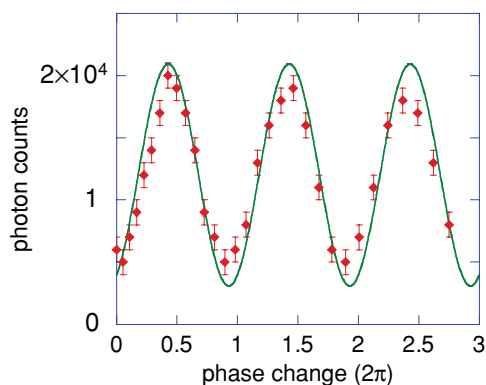


FIG. 4. (Color online) The number of 532-nm photons per second detected at the SPCM as a function of the introduced phase change. We observe sinusoidal variation with a large contrast. The solid line is a numerical calculation based on the measured power values and the beam sizes of the three Raman beams. The contrast of the theoretical curve is calculated without any adjustable parameters.

$W_s = 36 \mu\text{m}$ ,  $W_p = 33 \mu\text{m}$ , and  $W_a = 30 \mu\text{m}$ , respectively. The solid line in Fig. 4 is a numerical calculation based on the measured power values and the beam sizes. The only two fitting parameters are the unknown initial relative phase and an absolute vertical scaling; the contrast is calculated without any adjustable parameters. The large contrast of the experimental data and the good agreement with the theoretical calculation show that the three beams have almost perfect mutual-phase coherence. The data of Fig. 4 also demonstrate the ability for primitive waveform synthesis. At the peak of the interference fringes the three beams synthesize an AM-like wave form, whereas at the nodes they synthesize an FM-like wave form. The data take about 15 min to record, and the relative phase drift between the three beams is negligible during this period.

It is important to note that for the data of Fig. 4, we are not adjusting the Raman beam amplitudes to synthesize a prescribed time wave form. Instead, to maximize our signal, we work with the power values that we generate and only attenuate the pump beam by 60% to make the interfering paths more comparable. However, since the data of Fig. 4 prove good mutual coherence, we infer that by proper amplitude adjustment (simply by inserting appropriate neutral-density filters) we can synthesize any wave form within the capabilities of this spectrum. As an example, by making the Stokes and anti-Stokes light comparable in amplitude and much weaker than the pump, we can synthesize AM or FM wave forms. Figure 5 shows the synthesized temporal wave form when the three Raman amplitudes are adjusted to be equal and when the spectrum is phase locked. A near single-cycle optical wave form with a repetition period of 11 fs is formed. We note that, since the three CW beams are generated inside a HFC, they are predicted to have an absolute linewidth at the 1 kHz level [21]. The time wave form of Fig. 5 therefore is predicted to maintain its structure without significant change for about 1 ms.

To conclude, we have shown fully coherent CW light modulation at a frequency of 90 THz. Differing from earlier work, our experiment has demonstrated (1) significant anti-Stokes generation at a wavelength that is not resonant with

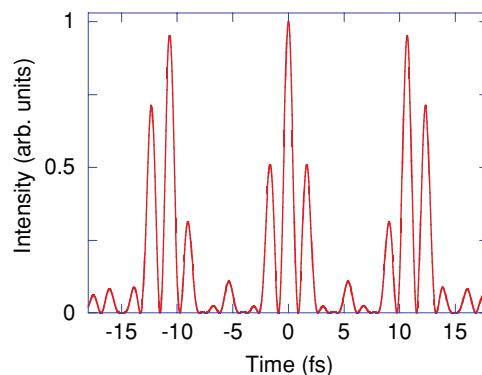


FIG. 5. (Color online) The intensity of the inferred synthesized temporal wave form when the spectrum is phase locked and the amplitudes of the three beams are adjusted to be equal. A near single-cycle optical wave form with a repetition period of 11 fs is formed. Since the absolute frequencies of the beams are not multiples of their frequency difference, the carrier-envelope phase changes at every period.

the cavity and (2) phase control and therefore a primitive form of wave-form synthesis in CW-stimulated Raman scattering. We view our experiment as the first step toward synthesizing arbitrary optical waveforms using CW spectral components. We note that a key limitation of our experiment is the optical power of the generated spectrum. Due to the low generated anti-Stokes power, the synthesized wave form of Fig. 5 has an average optical power of only a fraction of a milliwatt. Cooling the D<sub>2</sub> molecules to their rotational ground state (by using liquid nitrogen, for example) is predicted to increase the generated optical power by at least an order of magnitude [6].

Other future investigations will include operating near maximum coherence [22] or using a multiplicative technique [23] to increase the generated number of Raman beams and thereby increase the number of degrees of freedom in temporal wave-form synthesis.

We thank Prof. Mark Saffman's group for the loan of the SPCM and the optical spectrum analyzer. We also thank Dan Sikes and Nick Proite for experimental assistance and many helpful discussions. This work was supported by the National Science Foundation (NSF).

- 
- [1] A. V. Sokolov, D. D. Yavuz, D. R. Walker, G. Y. Yin, and S. E. Harris, *Phys. Rev. A* **63**, 051801(R) (2001).
  - [2] J. K. Brasseur, K. S. Repasky, and J. L. Carlsten, *Opt. Lett.* **23**, 367 (1998).
  - [3] L. S. Meng, P. A. Roos, and J. L. Carlsten, *Opt. Lett.* **27**, 1226 (2002).
  - [4] J. K. Brasseur, R. F. Teehan, P. A. Roos, B. Soucy, D. K. Neumann, and J. L. Carlsten, *Appl. Opt.* **43**, 1162 (2004).
  - [5] S. E. Harris and A. V. Sokolov, *Phys. Rev. Lett.* **81**, 2894 (1998).
  - [6] A. V. Sokolov, D. R. Walker, D. D. Yavuz, G. Y. Yin, and S. E. Harris, *Phys. Rev. Lett.* **85**, 562 (2000).
  - [7] M. Y. Shverdin, D. R. Walker, D. D. Yavuz, G. Y. Yin, and S. E. Harris, *Phys. Rev. Lett.* **94**, 033904 (2005).
  - [8] W. J. Chen *et al.*, *Phys. Rev. Lett.* **100**, 163906 (2008).
  - [9] A. H. Kung, in Fortieth Winter Colloquium on Physics of Quantum Electronics, Snowbird, Utah, 2010 (unpublished).
  - [10] S. Yoshikawa and T. Imasaka, *Opt. Commun.* **96**, 94 (1993).
  - [11] A. E. Kaplan, *Phys. Rev. Lett.* **73**, 1243 (1994).
  - [12] J. Q. Liang, M. Katsuragawa, F. Le Kien, and K. Hakuta, *Phys. Rev. Lett.* **85**, 2474 (2000).
  - [13] T. Suzuki, M. Hirai, and M. Katsuragawa, *Phys. Rev. Lett.* **101**, 243602 (2008).
  - [14] N. Zhavoronkov and G. Korn, *Phys. Rev. Lett.* **88**, 203901 (2002).
  - [15] S. I. Zaitso, H. Izaki, and T. Imasaka, *Phys. Rev. Lett.* **100**, 073901 (2008).
  - [16] S. Zaitso, C. Eshima, K. Ihara, and T. Imasaka, *J. Opt. Soc. Am. B* **24**, 1037 (2007).
  - [17] F. Couny, F. Benabid, and P. S. Light, *Phys. Rev. Lett.* **99**, 143903 (2007).
  - [18] J. T. Green, D. E. Sikes, and D. D. Yavuz, *Opt. Lett.* **34**, 2563 (2009).
  - [19] R. W. P. Drewer, J. L. Hall, F. V. Kowalski, J. Hough, G. M. Ford, A. J. Munley, and H. Ward, *Appl. Phys. B* **31**, 97 (1983).
  - [20] Z. Hsieh *et al.*, *Phys. Rev. Lett.* **102**, 213902 (2009).
  - [21] J. K. Brasseur, P. A. Roos, K. S. Repasky, and J. L. Carlsten, *J. Opt. Soc. Am. B* **16**, 1305 (1999).
  - [22] D. D. Yavuz, *Phys. Rev. A* **76**, 011805(R) (2007).
  - [23] D. D. Yavuz, D. R. Walker, M. Y. Shverdin, G. Y. Yin, and S. E. Harris, *Phys. Rev. Lett.* **91**, 233602 (2003).